RM L53I04

NACA

RESEARCH MEMORANDUM

ROCKET-MODEL INVESTIGATION TO DETERMINE THE HINGE-MOMENT AND NORMAL-FORCE PROPERTIES OF A FULL-SPAN, CONSTANT-CHORD, PARTIALLY BALANCED TRAILING-EDGE CONTROL ON A 60° CLIPPED DELTA WING BETWEEN MACH NUMBERS OF 0.50 AND 1.26

By C. William Martz and John W. Goslee

Langley Aeronautical Laboratory
Langley Field, Va.

NATIONAL ADVISORY COMMITTEE FOR AERONAUTICS

WASHINGTON

October 30, 1953

...SSIFICATION ... (or changed to Unclassified
...Y AUTHORITY Nasa Tech Rlb Announcement #120
(OFFICER AUTHORIZED TO CHANGE)
30 Jul 71
BY .....
.....
GRADE OF OFFICER MAKING CHANGE)
30 Nov 71
DATE

NATIONAL ADVISORY COMMITTEE FOR AERONAUTICS

RESEARCH MEMORANDUM

ROCKET-MODEL INVESTIGATION TO DETERMINE THE HINGE-MOMENT AND NORMAL-FORCE PROPERTIES OF A FULL-SPAN, CONSTANT-CHORD, PARTIALLY BALANCED TRAILING-EDGE CONTROL ON A 60° CLIPPED DELTA WING BETWEEN MACH NUMBERS OF 0.50 AND 1.26

By C. William Martz and John W. Goslee

SUMMARY

A free-flight investigation of a rocket-powered research model has been conducted to determine the hinge-moment and normal-force characteristics of a trailing-edge control on a delta wing between Mach numbers of 0.50 and 1.26. The model consisted of a cylindrical body with ogival nose and tail sections equipped with a cruciform arrangement of 60° swept-back clipped delta wings. The wing panels in one plane featured full-span, constant-chord, trailing-edge controls hinged at 40 percent control chord.

Results indicate that the hinge-line location of 40 percent control chord satisfactorily reduced the high hinge moments associated with plain-flap-type controls. This reduction was accompanied by increased hinge-moment nonlinearity. No appreciable difference in lifting effectiveness was noted between the control of the present test and the plain-flap-type control.

The center of pressure of the control-deflection forces was located at about 42 percent control chord at subsonic speeds and 51 percent control chord at supersonic speeds.

The center of pressure of the control-angle-of-attack forces had subsonic and supersonic locations of about 35 and 44 percent control chord, respectively.

INTRODUCTION

The desirability of trailing-edge plain-flap-type controls is evidenced by their use in many present-day aircraft despite the fact that in many cases the large hinge moments associated with this type of control at high speeds necessitate the use of a complicated control-boost system. The adequate effectiveness characteristics of these controls have been indicated in wind-tunnel results (refs. 1 and 2) and free-flight rocket tests (ref. 3). In an attempt to improve the hinge-moment characteristics of this type of control, an investigation was conducted through the use of a rocket-powered model incorporating 60° sweptback clipped delta wings with full-span, constant-chord trailing-edge controls hinged at 40 percent control chord. It was hoped that control overhang balance would provide reduced control hinge moments without adverse effects on control lifting effectiveness.

Control hinge moments were measured at various combinations of angle of attack (from ±4° at a Mach number of 1.26 to ±16° at a Mach number of 0.50) and control deflection (up to ±5°) at various Mach numbers between 0.5 and 1.26. Hinge-moment coefficients were obtained for combinations of angle of attack and control deflection within the test ranges by interpolating the measured data.

Lift-effectiveness data were also obtained for the entire model and for the controls.

Results are presented herein and are compared with linear theory and with other rocket-model data.

SYMBOLS

$\bar{c}$	wing mean aerodynamic chord, 1.492 ft
c_a	control-surface chord
S	total wing area in one plane, 2.847 sq ft
S_c	total exposed control area, sq ft
M_a	moment area of one control surface rearward of hinge line about the hinge line, 0.004828 cu ft

M_a' moment area of one control surface about control leading edge, cu ft

δ control-surface deflection at inboard end (trailing edge down, positive), deg

α angle of attack at model center of gravity, deg

M Mach number

ρ mass density of air, slugs/cu ft

V free-stream velocity, ft/sec

q dynamic pressure, $\rho V^2/2$, lb/sq ft

μ air-viscosity coefficient, slugs/ft-sec

R Reynolds number, $\rho\frac{\bar{c}V}{\mu}$

a_n model normal acceleration, g units

g acceleration of gravity, 32.2 ft/sec/sec

H hinge moment of one control about hinge line, in-lb

C_h control hinge-moment coefficient, $\frac{H/12}{2M_aq}$

C_h' control hinge-moment coefficient, $\frac{H/12}{2M_a'q}$

C_N total normal-force coefficient, $\frac{\text{Normal force on model}}{qS}$

$C_{h_\delta} = \frac{\partial C_h}{\partial \delta}$

$C_{h_\alpha} = \frac{\partial C_h}{\partial \alpha}$

$c.p._{\delta}$ chordwise center-of-pressure location of control force due to control deflection (measured from control leading edge)

$c.p._{\alpha}$ chordwise center-of-pressure location of control force due to angle of attack (measured from control leading edge)

$$C_{h_{\delta_a}} = \frac{\partial C_h'}{\partial \delta}$$

$$C_{h_{\alpha_a}} = \frac{\partial C_h'}{\partial \alpha}$$

$$C_{N_{\delta}} = \frac{\partial C_N}{\partial \delta}$$

$$C_{N_{\alpha}} = \frac{\partial C_N}{\partial \alpha}$$

MODEL

The hinge-moment research model used in this investigation consisted of a cylindrical body, with ogival nose and tail sections, equipped with a cruciform arrangement of 60° sweptback clipped delta wings. A drawing of the model showing overall dimensions is presented in figure 1 and photographs of the model are shown in figure 2.

The magnesium-alloy wings had an NACA 65A007 airfoil section. The wing panels in one plane featured full-span, 10-percent (exposed root) chord trailing-edge controls of modified double-wedge airfoil section. The controls had a maximum ratio of thickness to chord of 0.0968 over the inboard 80 percent control span. This ratio decreased to 0.0752 at the wing tip. The controls were hinged at 40.0 percent control chord and were of machined steel construction. No attempt was made to mass-balance the control system. Details of the wing and control are shown in figure 3.

INSTRUMENTATION

The model was equipped with an NACA telemetering system which transmitted the normal, transverse, and longitudinal acceleration, the static

and total pressure, the deflection angle and hinge moments of each control, the angle of attack, and the rate of pitch.

A control-position indicator and balances to measure control-hinge moments were constructed as integral parts of a power unit which was mounted in the rear part of the wing section of the model.

In addition to this model instrumentation, a radiosonde recorded atmospheric data at all flight altitudes shortly after the flight. Flight-path data were obtained with a radar tracking unit and a CW Doppler radar set was used to determine initial flight velocities. Photographic tracking was also employed to obtain visual records of the flight.

TECHNIQUE

The technique employed in this investigation consisted of mechanically pulsing the controls as elevators throughout the flight so that their deflection varied sinusoidally with time. The pulsing frequency was varied from 3.8 cps at a Mach number of 1.28 to 1.2 cps at a Mach number of 0.50 in an attempt to produce a nearly constant phase lag between the model pitching response and the control input. The control pulsing amplitude varied from $\pm 4^{\circ}$ to $\pm 5^{\circ}$ because of varying deflection in the control linkage throughout the speed range.

In addition to the aforementioned pitching oscillations, the response of the model involved small rolling and sideslip oscillations, the effects of which are believed to be negligible upon the results. This technique allowed the continuous measurement of hinge moments for each of two "identical" controls at various combinations of control deflection and angle of attack over the Mach number range of the investigation. Since the two sets of data were found to agree within experimental accuracy, the individual hinge-moment values were averaged for presentation.

All hinge-moment measurements were corrected for inertia effects of the control and control linkage caused by the pulsing motion. Measured values of control deflection were corrected for load deflection of the control system out to the inboard end of the controls.

Although a method of correcting the control-deflection data for control-surface twist was derived, it was decided that this correction would not be applied to the data in order to allow a more direct comparison with data from other sources. However, the amplitude of this twist correction is presented with a short discussion of the method in the appendix.

The test variation of Reynolds number with Mach number is presented in figure 4. All data were obtained in decelerated flight (0g to -3.1g).

ACCURACY

The subsequent information has been tabulated to indicate possible errors in basic measurements. These values are representative of the maximum instrument error in evaluating isolated data. In computations involving differences (such as slope evaluations), possible errors in the component quantities can be considered to be about one-half as large as those indicated.

Quantity	Error
Hinge moment, in-lb	±0.80
Control deflection, deg	±0.10
Angle of attack, deg	±0.26
Normal acceleration, g units	±0.40

RESULTS AND DISCUSSION

Hinge Moments

Hinge moments (in coefficient form) are presented in figures 5 and 6 as functions of control deflection and angle of attack, respectively. As a supplement to figures 5 and 6, simultaneous values of angle of attack, control-surface deflection, and control hinge moment are presented in table I.

Figure 5 shows data obtained at Mach numbers of 1.07 and 1.12 where intermittent failure of the telemeter apparatus resulted in data recovery only at the larger positive angles of attack. The data are presented, therefore, as a function of control deflection. The solid-line curve connecting the data points represents the measured hinge-moment data, and the straight-line curves which connect end points of equal angle of attack were constructed by assuming C_{h_δ} to be constant with δ at individual angles of attack so as to obtain some indication of the separate effects of α and δ on hinge moments. Since this method of straight-line fairing could introduce errors at the higher angles of attack (because of an increase in hinge-moment nonlinearity), the results obtained from this fairing should be considered mainly as trends.

Hinge-moment data at other Mach numbers (fig. 6) were obtained more fully in that information of complete cycles of angle of attack and control-surface deflection was available. This information was obtained by plotting C_h as a function of control deflection, connecting points of equal angle of attack with straight lines (as in fig. 5) and cross-plotting the faired C_h intercepts at various deflections as a function of angle of attack.

Hinge moments can be determined for all combinations of angle of attack and control deflection within the data loops at each Mach number by linear interpolation between the lines of constant control deflection. Similarly, reasonable extrapolation yields values outside the data loops.

The hinge-moment parameter C_{h_α} is indicated by the slope of the constant-deflection curves for various control deflections. Negative values of C_{h_α} indicate the control to be statically stable with angle of attack (i.e., the center of pressure of the angle-of-attack load on the control is behind the hinge line), and positive slopes indicate the control to be statically unstable (center of pressure ahead of the hinge line).

The variation of C_h with α is seen to be fairly linear up to values of α of $\pm 3^\circ$ or $\pm 4^\circ$ at all Mach numbers and control deflections presented. At those Mach numbers where the higher angle-of-attack data are available, C_{h_α} first decreases as α is increased (to about $\pm 8^\circ$) and then increases for values of α larger than $\pm 8^\circ$. These nonlinearities result from small variations in control-center-of-pressure location, the effect being magnified over the plain-flap case because of the relatively high degree of aerodynamic balance obtained with the present test control. Control deflection is seen to have little effect upon C_{h_α} except between Mach numbers of 0.90 and 0.96 where the values are more negative when α and δ are of the same sign and are less negative when α and δ are of opposite sign. Some of these effects can be seen in figure 7 which presents values of C_{h_α} as a function of Mach number for control deflections of 0° and 4° as obtained for values of α near zero and for the undeflected control as obtained over an angle-of-attack range of $\pm 6^\circ$. These curves are seen to be almost constant at subsonic and supersonic speeds with an abrupt shift (first positive and then negative) as Mach number increases from 0.875 to 0.975. Values of C_{h_α} are fairly small over the Mach number range and, as stated before, are affected very little by control deflection. Although increasing the range of α from 0° to $\pm 6^\circ$ decreases the values of C_{h_α} about 45 percent (data available

at subsonic speeds only), the actual magnitude of this decrease is rather small. Shown for comparison on figure 7 are data obtained from a missile configuration employing 70° sweptback delta wings with constant-chord trailing-edge controls hinged at 44.4 percent control chord (ref. 1). As would be expected, these values are somewhat less negative than the present test values (extrapolated) because of the more rearward hinge-line location.

Concerning the effects of control deflection on hinge moments, the reader can return to figure 6 where values of C_{h_δ} can be determined at various angles of attack by cross-plotting the intercepts of the constant-control-deflection curves. The values of C_{h_δ} are negative at all Mach numbers, thus indicating that the control is statically stable with control deflection (i.e., the center of pressure of the control-deflection loading is behind the hinge line). These values are presented in figure 8 as a function of Mach number for angles of attack of 0° and ±6°. The curves are somewhat typical with relatively constant values up to the transition region ($0.85 < M < 1.0$), where abrupt negative increases occur, and with slowly decreasing negative values at supersonic speeds. Angle of attack appears to have very little effect on C_{h_δ} except in the transition region.

Although the supersonic values of C_{h_δ} may appear large at first glance (on the order of -0.02 to -0.03), it should be remembered that the hinge-moment coefficients were based upon the control-moment area behind the hinge line and, when converted to hinge moments for comparison with data from unbalanced controls, would have an effective reduction of about 65 percent. Also shown in figure 8 are values of C_{h_δ} obtained from reference 1 for a configuration previously described. Again, the values are somewhat less negative than the present test values (extrapolated) as would be expected from the more rearward location of the hinge line.

In an attempt to predict the hinge-moment characteristics (with respect to both angle of attack and control deflection) of a control similar to that of the present investigation for various hinge-line locations, hinge-moment coefficients (based on the moment area of the control about the control leading edge) were determined for the present test configuration (extrapolated from $M = 1.26$ to $M = 1.3$) and for the configurations of references 1 to 3. These data are presented in figure 9 at a Mach number of 1.3 as a function of chordwise hinge-line location. The two sets of data are shown connected by straight lines. The slopes of these lines are indicative of the control-normal-force characteristics and the intersections of these lines with the zero abscissa yield the chordwise locations of the control centers of pressure. It should be

pointed out that the straight-line fairing of these curves effectively assumes that the lift-per-unit-control area produced on each control is identical for all configurations. Since the validity of this assumption is questionable in some cases, and because it was realized that the errors involved would have a larger effect on the slopes of these lines than on the intersections with the zero abscissa, it was decided that this type of analysis would be used in determining center-of-pressure locations only. Thus, from curves similar to those of figure 9 which were obtained with the combined data of the present report and references 2 and 3, center-of-pressure locations were determined for Mach numbers between 0.7 and 1.3 and are presented in figure 10 as a function of Mach number.

The control chordwise center of pressure due to control deflection $c.p._{\delta}$ is seen to have two principal locations over the speed range: a forward location of about $42\frac{1}{2}$ percent control chord for Mach numbers up to 0.975 and a rearward location of about $51\frac{1}{2}$ percent control chord for Mach numbers greater than 1.03, with a smooth transition between Mach numbers of 0.975 and 1.03. This supersonic value of $51\frac{1}{2}$ percent agrees fairly well with values of 48 to 49 percent as predicted by linearized theory for a similar control not having control cutouts (from rectangular wing data of ref. 4). As would be expected, the control cutouts of the present test and of reference 1 have shifted the control center of pressure due to deflection rearward.

The chordwise control center of pressure associated with angle of attack $c.p._{\alpha}$ also has two principal locations: 35 percent chord for Mach numbers less than 0.95 and 44 percent chord for Mach numbers greater than 1.03, the 9-percent rearward shift in $c.p._{\alpha}$ between Mach numbers of 0.95 and 1.03 being smooth. The supersonic value of $c.p._{\alpha}$ predicted by linear theory for a similar control with no cutouts and with the control tip not clipped was determined from reference 5 to be 48 percent control chord. Although this value would be decreased slightly for the clipped tips and increased slightly by the cutouts, agreement with the 44-percent value of figure 10 is believed to be fairly good.

Normal Force

Figure 11 presents the variation of normal-force coefficient with control deflection at various angles of attack for $M = 1.26$. These results were obtained from measured normal accelerations of the model in flight. The irregular curve represents the measured data and the lines of constant angle of attack are linear curves faired between points of

equal angle of attack on the irregular curve. The slopes of the constant-angle-of-attack lines are equal to C_{N_δ} and values of C_{N_α} are obtained by cross-plotting the C_N intercepts of the faired curves at any control deflection. Since the faired curves are nearly parallel and equally spaced, values of C_{N_α} and C_{N_δ} are independent of angle of attack and control deflection. These results are presented in figures 12 and 13(a) as a function of Mach number. Other experimental results of C_{N_α} for a similar model (ref. 6) are shown in figure 12 for comparison.

In order to compare directly the control-force characteristics of the present test model with other experimental results, the normal-force coefficient based on exposed control area $C_{N_\delta}\frac{S}{S_c}$ was calculated from the present test results and for the configurations of reference 1 (previously described) and reference 3 which is a tailless airplane with 60° sweptback wings and trailing-edge controls of the constant-chord plain-flap type. This information is presented in figure 13(b) and indicates that no appreciable difference in lifting effectiveness exists between the plain-flap control and the flap controls with overhang balance.

CONCLUSIONS

A free-flight investigation of a rocket-powered research model has been made to determine the hinge-moment and normal-force properties of a full-span, constant-chord trailing-edge control (hinge line at 40 percent control chord) on a 60° clipped delta wing between Mach numbers of 0.50 and 1.26. The following conclusions are presented:

1. Control hinge moments were relatively small throughout the speed range for all combinations of control deflection and angle of attack tested.

2. The considerable amount of aerodynamic balance provided by rearward location of the control hinge line was obtained at the expense of increased hinge-moment nonlinearity.

3. The use of control overhang balance appeared to have no appreciable effect on control lifting effectiveness.

4. The center of pressure of the control-deflection loading had a subsonic location of about $42\frac{1}{2}$ percent control chord and a supersonic location of about $51\frac{1}{2}$ percent control chord.

5. The center of pressure of the control-angle-of-attack loading was located at about 35 percent control chord at subsonic speeds and at about 44 percent control chord at supersonic speeds.

Langley Aeronautical Laboratory,
National Advisory Committee for Aeronautics,
Langley Field, Va., August 21, 1953.

APPENDIX

CONTROL TWIST CORRECTION

As previously stated in a previous section of the present report, a method of correcting the control-deflection data for control-surface twist has been derived. Experimental data requirements for the application of this method include a static-twist calibration of the control-surface and aerodynamic hinge-moment data as a function of uncorrected (for twist) control deflection and angle of attack.

The method includes two basic assumptions: that control bending has a negligible effect on control twist and that the time rate of twisting is low enough to negate twisting moments due to inertial forces. Although the method does not require a simplified type of assumed spanwise control loading, the assumption that the loads due to angle of attack, control deflection, and out-of-trim were uniformly distributed along the span simplified the method for use with the present test results without introducing appreciable errors.

The twist corrections for the present test results are indicated by the equation

$$\frac{\delta_e}{\delta} = \frac{\partial H}{\partial \delta} - \left[\frac{R}{2} - 40.10 \left(1 - \sqrt{2.400 \frac{\delta_e}{\delta} + 0.0001555R^2 - 0.02494R - 1.400} \right) \right]^{-1}$$

where

δ_e/δ twist correction factor,

$$\frac{\text{Mean control deflection of twisted surface}}{\text{Deflection at inboard end of control}}$$

$\partial H/\partial \delta$ rate of change of hinge moment with deflection at inboard end of control

$$R = \frac{H_\alpha + H_o}{\delta}$$

H_α control hinge moment resulting from angle of attack

H_o out-of-trim control hinge moment

In order to illustrate the amplitude of this correction, values of δ_e/δ for the present test configuration were evaluated for standard sea-level conditions and for zero out-of-trim hinge moment, the latter condition allowing R (and, hence, δ_e/δ) to be expressed as a function of α/δ. These values are presented in figure 14 as a function of Mach number for several values of α/δ.

The curves are seen to be similar with no appreciable control twist indicated up to M = 0.9. As the Mach number increases from 0.9 to 1.0, the twist correction factor abruptly decreases from about 0.98 to 0.89, the latter value indicating an 11-percent decrease in effective deflection due to control twist. For Mach numbers larger than 0.94, the parameter α/δ plays an increasingly larger part in determining the amount of control twist. At M = 1.3, the decrease in effective deflection varies from about 8 to 16 percent at α/δ is varied from -1 to 1.

REFERENCES

1. Mason, Maxwell, and Miller, Robert C.: Wind-Tunnel Test of 11 Per Cent Scale Semispan Models of the Douglas Nike 484 Missile. Rep. No. SWT 12-8, Jet Propulsion Lab., C.I.T., 1950.

2. Boyd, John W.: Aerodynamic Characteristics of Two 25-Percent-Area Trailing-Edge Flaps on an Aspect Ratio 2 Triangular Wing at Subsonic and Supersonic Speeds. NACA RM A52D01c, 1952.

3. Mitcham, Grady L., Crabill, Norman L., and Stevens, Joseph E.: Flight Determination of the Drag and Longitudinal Stability and Control Characteristics of a Rocket-Powered Model of a 60° Delta-Wing Airplane From Mach Numbers of 0.75 to 1.70. NACA RM L51I04, 1951.

4. Harmon, Sidney M.: Stability Derivatives at Supersonic Speeds of Thin Rectangular Wings With Diagonals Ahead of Tip Mach Lines. NACA Rep. 925, 1949. (Supersedes NACA TN 1706.)

5. Tucker, Warren A.: Characteristics of Thin Triangular Wings With Constant-Chord Full-Span Control Surfaces at Supersonic Speeds. NACA TN 1601, 1948.

6. Martz, C. William, Church, James D., and Goslee, John W.: Rocket-Model Investigation To Determine the Force and Hinge-Moment Characteristics of a Half-Delta Tip Control on a 59° Sweptback Delta Wing Between Mach Numbers of 0.55 and 1.43. NACA RM L52H06, 1952.

TABLE I.- EXPERIMENTAL ANGLE-OF-ATTACK, CONTROL-SURFACE-DEFLECTION, AND CONTROL-HINGE-MOMENT DATA

M = 1.26			M = 1.12			M = 1.06			M = 0.96			M = 0.94		
δ	α	C_h	δ	α	C_h	δ	α	C_h	δ	α	C_h	δ	α	C_h
1.57	-3.04	-0.0011	-3.89	3.79	0.0809	-4.02	5.55	0.0894	-1.18	-7.89	0.0617	2.27	-7.61	-0.0663
.36	-2.97	.0180	-3.37	5.23	.0575	-3.60	6.77	.0701	-2.05	-7.23	.0870	1.31	-8.42	-.0371
-.67	-2.75	.0375	-2.54	6.46	.0314	-3.06	7.75	.0516	-2.86	-6.15	.1048	.45	-8.94	.0075
-1.70	-2.31	.0543	-1.57	7.29	.0063	-2.34	8.39	.0326	-3.48	-4.83	.1123	-.47	-8.77	.0382
-2.62	-1.60	.0684	-.52	7.86	-.0168	-1.38	8.58	.0128	-4.16	-3.10	.1158	-1.53	-8.40	.0540
-3.37	-.88	.0804	.42	7.94	-.0426	-.67	8.45	-.0074	-4.50	-1.28	.1200	-2.38	-7.76	.0658
-3.96	.00	.0867	1.63	7.68	-.0690	.16	8.05	-.0289	-4.43	.77	.1174	-3.32	-6.39	.0730
-4.27	.93	.0896	2.55	6.98	-.0899	.97	7.58	-.0487	-4.46	2.52	.1107	-3.89	-5.51	.0831
-4.35	1.76	.0862	3.33	5.88	-.1055	1.83	6.87	-.0680	-4.30	4.33	.1062	-4.39	-3.70	.0835
-4.25	2.67	.0778	3.95	4.74	-.1135				-3.82	5.82	.0958	-4.53	-1.79	.0763
-3.94	3.40	.0648	4.44	3.56	-.1141				-3.21	7.10	.0710	-4.54	-.08	.0707
-3.33	3.95	.0477							-2.31	8.30	.0538	-4.45	1.93	.0694
-2.46	4.41	.0314							-1.62	8.95	.0311	-4.19	3.73	.0866
-1.42	4.59	.0134							-.36	9.40	.0015	-3.51	5.34	.0916
-.42	4.53	-.0067							.34	9.06	-.0304	-2.76	6.85	.0767
.57	4.26	-.0270							1.40	8.82	-.0564	-1.89	8.21	.0520
1.67	3.60	-.0461							2.23	7.90	-.0820	-1.02	9.10	.0123
2.70	2.86	-.0634							3.03	6.81	-.1028	-.28	9.56	-.0100
3.46	2.08	-.0770							3.68	5.57	-.1160	1.05	9.59	-.0125
4.07	1.02	-.0848							4.24	3.76	-.1167	2.00	9.31	-.0203
4.48	-.18	-.0878							4.53	1.90	-.1197	2.90	8.69	-.0298
4.67	-1.21	-.0833							4.63	.10	-.1178	3.65	7.80	-.0359
4.61	-2.27	-.0724							4.58	-1.80	-.1064	4.36	6.52	-.0416
4.30	-3.12	-.0579							4.26	-3.76	-.1015	4.76	4.99	-.0440
3.68	-3.91	-.0405							3.86	-5.25	-.0977	4.98	3.02	-.0388
2.90	-4.42	-.0215							3.18	-6.55	-.0820	4.87	1.19	-.0354
1.98	-4.69	-.0015							2.27	-7.61	-.0627	4.64	-.73	-.0348
0.83	-4.62	.0178							1.31	-8.42	-.0351	4.44	-2.88	-.0426
									.45	-8.94	.0071	3.83	-4.54	-.0498
									-.47	-8.77	.0361	3.17	-6.26	-.0462
									-1.03	-8.40	.0511	2.33	-7.60	-.0238
									-2.38	-7.76	.0622	1.37	-8.59	-.0120
									-3.32	-6.39	.0690	.47	-9.20	-.0050
												-.44	-9.51	.0055
												-1.38	-9.43	.0125

TABLE I.- EXPERIMENTAL ANGLE-OF-ATTACK, CONTROL-SURFACE-DEFLECTION, AND CONTROL-HINGE-MOMENT DATA - Continued

M = 0.90			M = 0.86			M = 0.80		
δ	α	C_h	δ	α	C_h	δ	α	C_h
0.20	11.41	0.0088	-4.25	-7.40	0.0191	4.88	11.13	-0.0098
1.10	11.12	-.0003	-4.62	-5.30	.0212	5.11	9.95	-.0122
1.96	10.36	-.0074	-4.97	-3.29	.0135	5.14	8.95	-.0144
2.80	9.39	-.0223	-5.03	-1.17	.0181	5.01	7.60	-.0115
3.54	7.89	-.0233	-4.86	1.00	.0266	4.82	6.33	-.0095
4.21	6.05	-.0162	-4.50	3.10	.0353	4.35	4.51	-.0040
4.59	4.13	-.0095	-4.04	4.93	.0348	3.77	2.68	-.0039
4.93	1.98	-.0066	-3.39	6.93	.0331	2.98	1.20	-.0065
5.14	-.28	-.0182	-2.78	8.64	.0198	2.15	-.48	-.0085
5.09	-2.70	-.0400	-1.91	10.03	.0142	1.21	-2.29	-.0137
4.82	-5.04	-.0548	-1.16	10.89	.0003	.38	-4.07	-.0120
4.37	-6.98	-.0752	-.19	11.35	-.0132	-.48	-5.40	-.0092
3.93	-8.64	-.0750	.67	11.83	-.0215	-1.43	-6.70	.0015
3.27	-10.19	-.0663	1.62	11.82	-.0302	-2.29	-7.80	.0069
2.56	-11.35	-.0357	2.55	11.48	-.0363	-3.04	-8.57	.0078
1.71	-12.06	-.0256	3.22	10.70	-.0434	-3.73	-9.08	.0060
.82	-12.23	-.0081	3.87	9.73	-.0409	-4.20	-9.46	.0046
-.14	-12.09	.0020	4.38	8.56	-.0392	-4.62	-9.46	.0046
-1.07	-11.57	.0015	4.80	6.82	-.0371	-4.86	-9.21	.0094
-1.95	-10.50	.0088	5.04	5.17	-.0259	-4.93	-8.56	.0158
-2.69	-8.82	.0154	5.11	3.65	-.0199	-4.80	-7.64	.0166
-3.48	-6.93	.0227	5.06	1.69	-.0208	-4.55	-6.66	.0138
-4.10	-4.99	.0128	4.84	-.07	-.0242	-4.02	-5.38	.0061
-4.58	-2.77	.0029	4.41	-1.96	-.0290	-3.51	-4.05	.0022
-4.80	-.18	.0189	3.73	-3.90	-.0323	-2.88	-2.67	.0021
-4.89	2.11	.0375	3.16	-5.26	-.0289	-2.04	-1.05	.0032
-4.82	4.47	.0464	2.46	-6.61	-.0223	-1.27	.49	.0041
-4.48	6.77	.0702	1.47	-7.86	-.0163	-.38	1.88	.0058
-3.99	8.78	.0783	.70	-8.63	-.0100	.52	3.35	.0056
-3.40	10.48	.0778	-.20	-9.42	-.0036	1.41	4.96	.0034
-2.77	11.92	.0538	-1.09	-10.05	-.0023	2.23	5.99	.0020
-1.92	12.88	.0323	-1.90	-10.39	.0011	2.95	7.04	-.0086
-1.23	13.52	.0180	-2.65	-10.37	.0059	3.58	7.85	-.0127
-.24	13.68	.0088	-3.38	-10.35	.0091	4.13	8.51	-.0122
.64	13.35	.0011	-3.96	-9.85	.0134	4.56	8.72	-.0134
			-4.41	-9.08	.0206	4.87	8.85	-.0140
			-4.60	-7.58	.0230	5.08	8.73	-.0143
			-4.77	-6.08	.0200	5.18	8.34	-.0126
						5.15	7.59	-.0123

TABLE I.- EXPERIMENTAL ANGLE-OF-ATTACK, CONTROL-SURFACE-DEFLECTION, AND CONTROL-HINGE-MOMENT DATA - Concluded

M = 0.75			M = 0.70			M = 0.60			M = 0.50		
δ	α	C_h	δ	α	C_h	δ	α	C_h	δ	α	C_h
-4.52	-9.09	0.0125	-2.39	-6.60	-0.0028	-4.28	5.50	0.0110	-3.96	12.15	0.0100
-4.67	-7.54	.0146	-2.96	-7.50	.0010	-4.02	7.01	.0108	-3.73	12.61	.0112
-4.73	-6.60	.0128	-3.59	-8.15	.0041	-3.65	8.44	.0089	-3.47	12.99	.0091
-4.73	-5.24	.0032	-4.07	-8.69	.0064	-3.28	9.85	.0095	-3.24	13.13	.0091
-4.68	-3.94	.0036	-4.47	-8.79	.0053	-2.89	11.10	.0159	-2.89	13.18	.0097
-4.51	-2.58	.0043	-4.61	-8.96	.0053	-2.45	12.25	.0196	-2.62	13.03	.0085
-4.10	-1.18	.0079	-4.75	-8.84	.0053	-2.00	13.30	.0165	-2.29	12.93	.0082
-3.61	.54	.0113	-4.76	-8.46	.0068	-1.54	14.15	.0143	-1.98	12.68	.0048
-3.03	1.93	.0155	-4.74	-7.97	.0077	-1.05	14.81	.0153	-1.62	12.17	-.0006
-2.37	3.53	.0168	-4.65	-7.19	.0056	-.51	15.33	.0275	-1.32	11.75	-.0006
-1.61	5.02	.0145	-4.39	-6.45	-.0022	-.10	15.69	.0234	-.93	11.26	-.0012
-.84	6.23	.0107	-3.89	-5.65	-.0039	.41	15.88	.0227	-.53	10.40	-.0036
-.14	7.36	.0056	-3.43	-4.40	-.0043	.92	15.87	.0198	-.23	9.55	-.0073
.63	8.46	.0036	-2.77	-3.14	-.0039	1.40	15.69	.0186	.14	8.69	-.0070
1.45	9.35	.0032	-2.19	-2.07	-.0044	1.87	15.35	.0155	.49	7.66	-.0070
2.12	9.93	.0027	-1.52	-.98	-.0028	2.46	14.88	.0116	.88	6.89	-.0070
2.82	10.48	-.0015	-.79	.40	-.0025	2.78	14.29	.0079	1.16	5.58	-.0079
3.55	10.50	-.0034	.11	1.39	-.0019	3.17	13.50	.0033	1.55	4.82	-.0100
4.11	10.50	-.0067	.68	2.60	-.0015	3.54	12.58	-.0050	1.89	3.73	-.0109
4.54	10.19	-.0106	1.30	3.61	-.0009	3.90	11.05	-.0085	2.28	2.85	-.0136
4.82	9.53	-.0132	1.95	4.50	-.0021	4.22	9.85	-.0134	2.58	1.62	-.0182
5.04	8.62	-.0155	2.59	5.23	-.0022	4.46	8.54	-.0176	2.91	.82	-.0209
5.12	7.48	-.0155	3.19	6.29	-.0040	4.65	6.67	-.0176	3.18	-.34	-.0248
5.14	6.33	-.0119	3.66	6.81	-.0085	4.83	5.18	-.0165	3.48	-1.26	-.0294
4.98	4.76	-.0085	4.12	7.31	-.0127	5.01	3.50	-.0188	3.75	-2.09	-.0333
4.75	3.33	-.0113	4.48	7.61	-.0141	5.12	1.81	-.0221	3.98	-3.07	-.0390
4.36	1.72	-.0139	4.76	7.74	-.0158	5.05	.26	-.0238	4.20	-4.11	-.0397
3.95	.23	-.0175	4.99	7.77	-.0161	5.08	-1.49	-.0281	4.37	-5.22	-.0415
3.35	-1.30	-.0206	5.06	7.57	-.0161	4.98	-3.16	-.0341	4.60	-6.02	-.0442
2.68	-2.84	-.0222	5.08	7.24	-.0161	4.91	-4.93	-.0358	4.75	-7.24	-.0448
1.90	-4.63	-.0220	5.06	6.69	-.0114	4.72	-6.69	-.0376	4.87	-7.92	-.0448
1.15	-5.75	-.0175	4.92	6.02	-.0076	4.47	-8.28	-.0370	5.00	-9.08	-.0433
.44	-7.24	-.0107	4.76	5.22	-.0068	4.31	-9.79	-.0378	5.09	-9.66	-.0457
-.36	-8.37	-.0071	4.43	4.24	-.0080	3.98	-11.49	-.0417	5.16	-10.52	-.0472
-1.16	-9.32	-.0112	4.05	3.27	-.0084	3.65	-12.58	-.0380	5.19	-11.14	-.0496
-1.90	-9.85	-.0100	3.63	2.24	-.0107	3.30	-13.60	-.0397	5.17	-11.94	-.0496
-2.54	-10.52	-.0085	3.10	1.02	-.0123	2.82	-14.57	-.0500	5.20	-12.48	-.0515
-3.20	-10.73	-.0069	2.56	-.04	-.0124	2.42	-15.36	-.0488	5.07	-13.03	-.0524
-3.71	-10.82	-.0041	1.91	-1.12	-.0132	1.95	-16.04	-.0484	5.15	-13.43	-.0539
-4.23	-10.42	-.0020	1.27	-2.14	-.0147	1.40	-16.58	-.0484	4.98	-13.79	-.0578
-4.68	-9.71	-.0014	.66	-3.12	-.0145	.93	-16.91	-.0484	4.87	-14.09	-.0572
-4.63	-9.04	.0067	.01	-4.42	-.0127	.32	-17.08	-.0469	4.72	-14.28	-.0566
-4.73	-7.88	.0137	-.65	-5.18	-.0123	-.15	-17.08	-.0422	4.64	-14.40	-.0566
-4.72	-6.51	.0100	-1.27	-5.96	-.0102	-.67	-16.90	-.0389	4.46	-14.40	-.0563
-4.73	-5.52	.0023	-1.86	-6.73	-.0067	-1.08	-16.60	-.0382	4.19	-14.37	-.0563
-4.68	-4.87	.0028	-2.42	-7.32	-.0019	-1.61	-16.11	-.0353	3.90	-14.28	-.0560
			-3.02	-7.64	.0002	-2.22	-15.49	-.0304	3.66	-14.14	-.0542
			-3.53	-7.73	.0018	-2.52	-14.66	-.0271	3.33	-13.96	-.0554
			-4.01	-7.90	.0033	-2.98	-13.66	-.0139	3.13	-13.71	-.0536
			-4.36	-7.80	.0064	-3.31	-12.53	-.0068	2.72	-13.40	-.0451
			-4.56	-7.52	.0068	-3.62	-11.29	-.0103	2.41	-12.99	-.0427
						-4.05	-9.42	-.0091	1.95	-12.51	-.0390
						-4.32	-8.10	-.0070	1.59	-11.67	-.0390
						-4.53	-6.32	-.0087	1.24	-11.16	-.0400
						-4.73	-4.47	-.0074	.88	-10.42	-.0336
						-4.85	-2.93	-.0052	.48	-9.53	-.0321
						-4.96	-1.21	-.0010	.13	-8.69	-.0294
						-4.97	.47	.0017	-.26	-7.54	-.0303
						-4.97	1.99	.0058	-.60	-6.73	-.0294
						-4.91	3.54	.0097	-.96	-5.75	-.0294
						-4.79	5.48	.0108	-1.28	-4.89	-.0275
						-4.63	7.04	.0116	-1.62	-3.55	-.0254
						-4.34	8.34	.0095	-2.00	-2.72	-.0254
						-4.05	9.72	.0108	-2.29	-1.62	-.0200
						-3.79	11.11	.0157	-2.61	-.73	-.0173
						-3.43	12.43	.0207	-2.89	.28	-.0142
						-3.03	13.69	.0246	-3.21	1.33	-.0112
									-3.43	2.22	-.0082
									-3.68	3.23	-.0030
									-3.85	4.21	-.0006
									-4.10	5.19	.0018
									-4.34	6.14	.0030
									-4.46	7.09	.0036
									-4.61	8.14	.0036
									-4.73	9.03	.0048
									-4.85	9.97	.0064
									-4.92	10.51	.0082
									-4.97	11.46	.0088
									-4.98	12.11	.0091
									-5.00	12.85	.0115
									-4.93	13.39	.0182

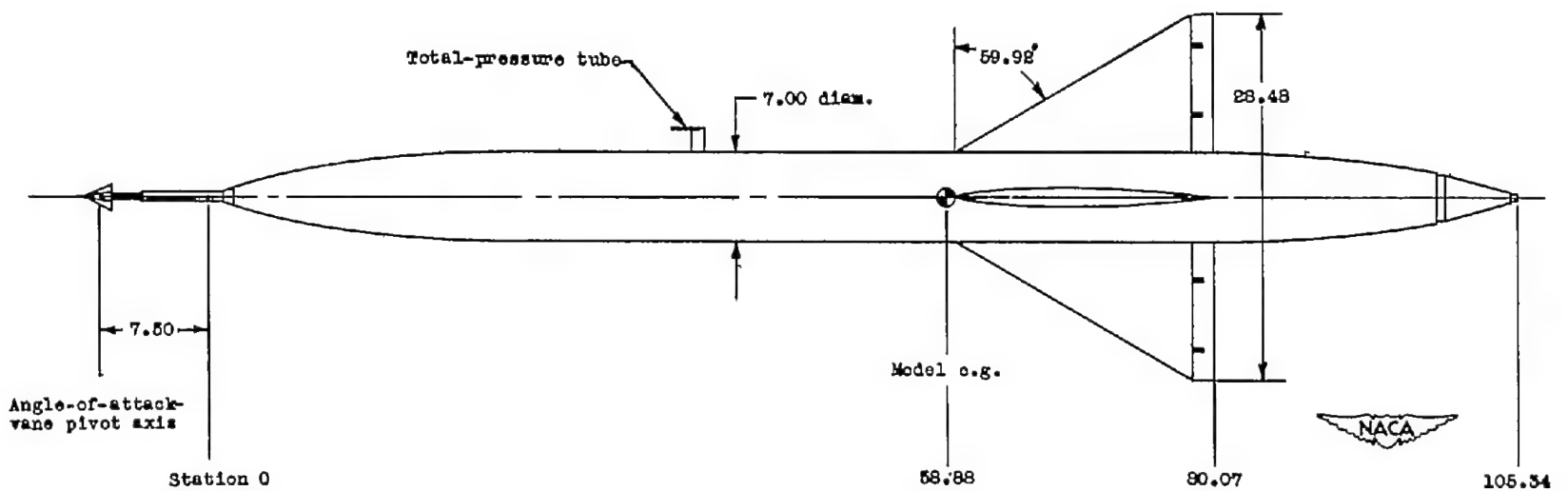

Model weight, 119.125 pounds

Figure 1.- Plan view of test vehicle. All dimensions are in inches.

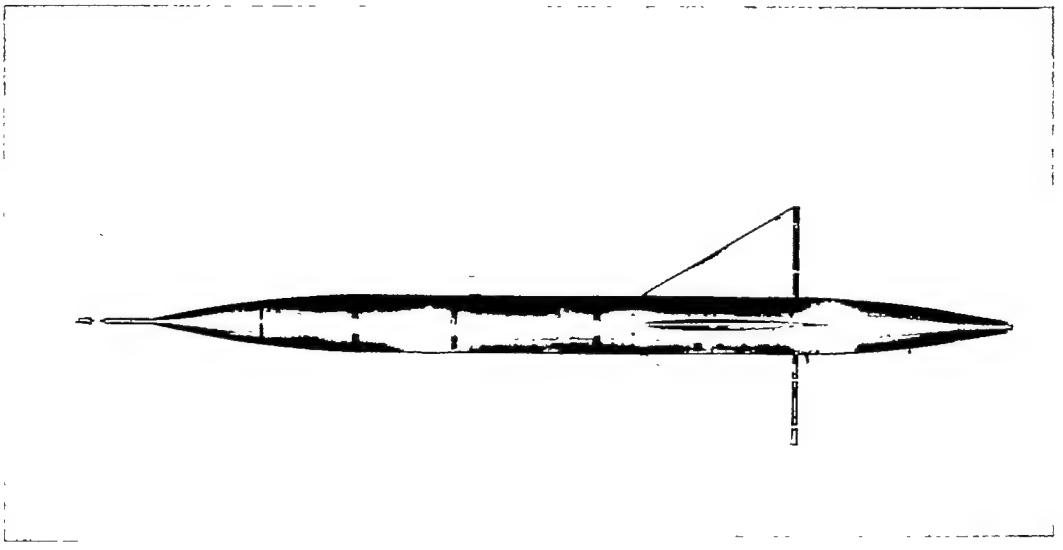

L-72391.1

(a) Top view.

L-72390.1

(b) Side view.

Figure 2.- Photographs of test vehicle.

L-72392.1

(c) Control details.

L-73006.1

(d) Preparatory to launching.

Figure 2.- Concluded.

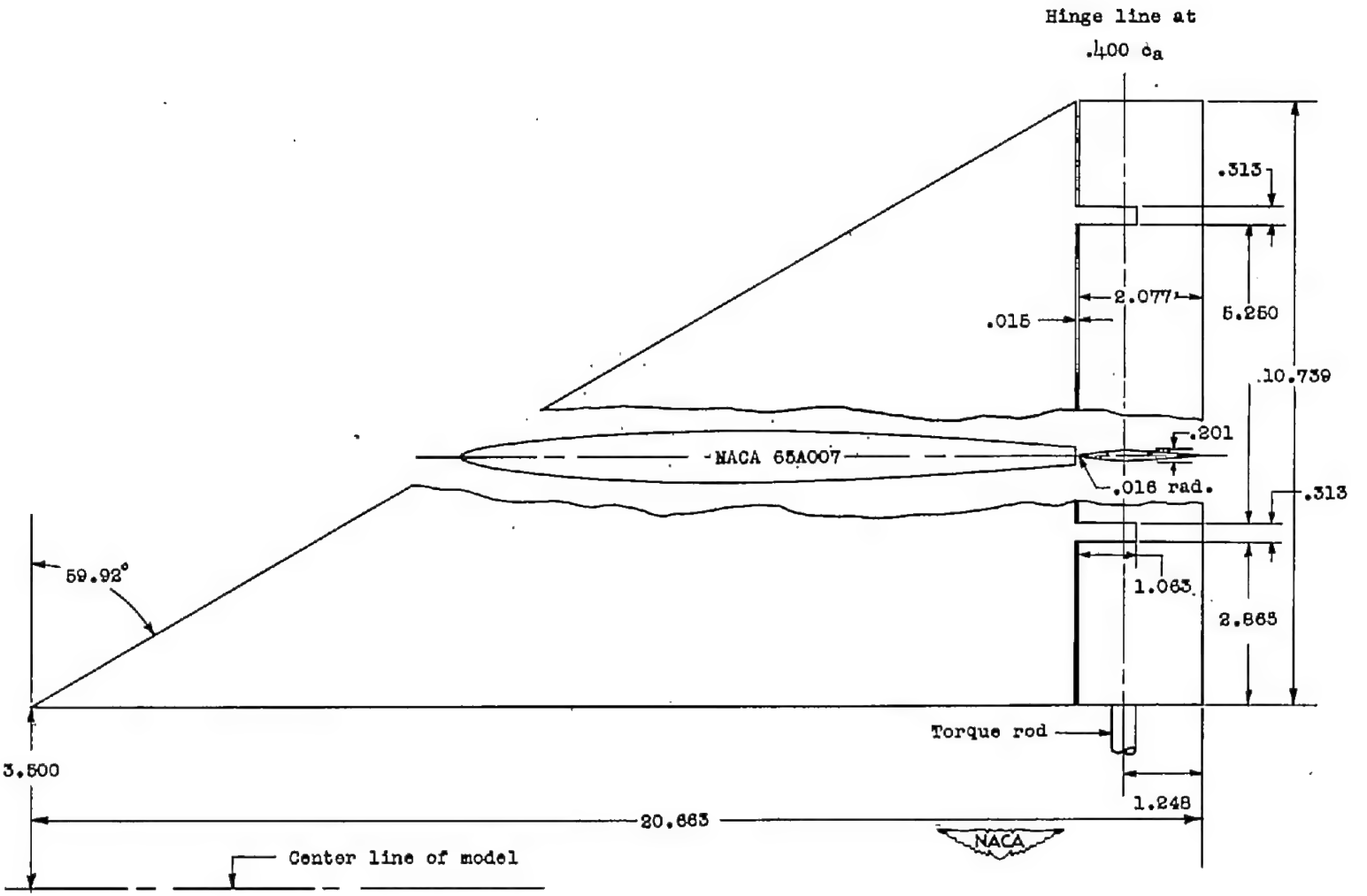

Figure 3.- Details of wing and control. Control maximum thickness is constant over inboard 80 percent span and tapers to 0.156 at tip. All dimensions are in inches.

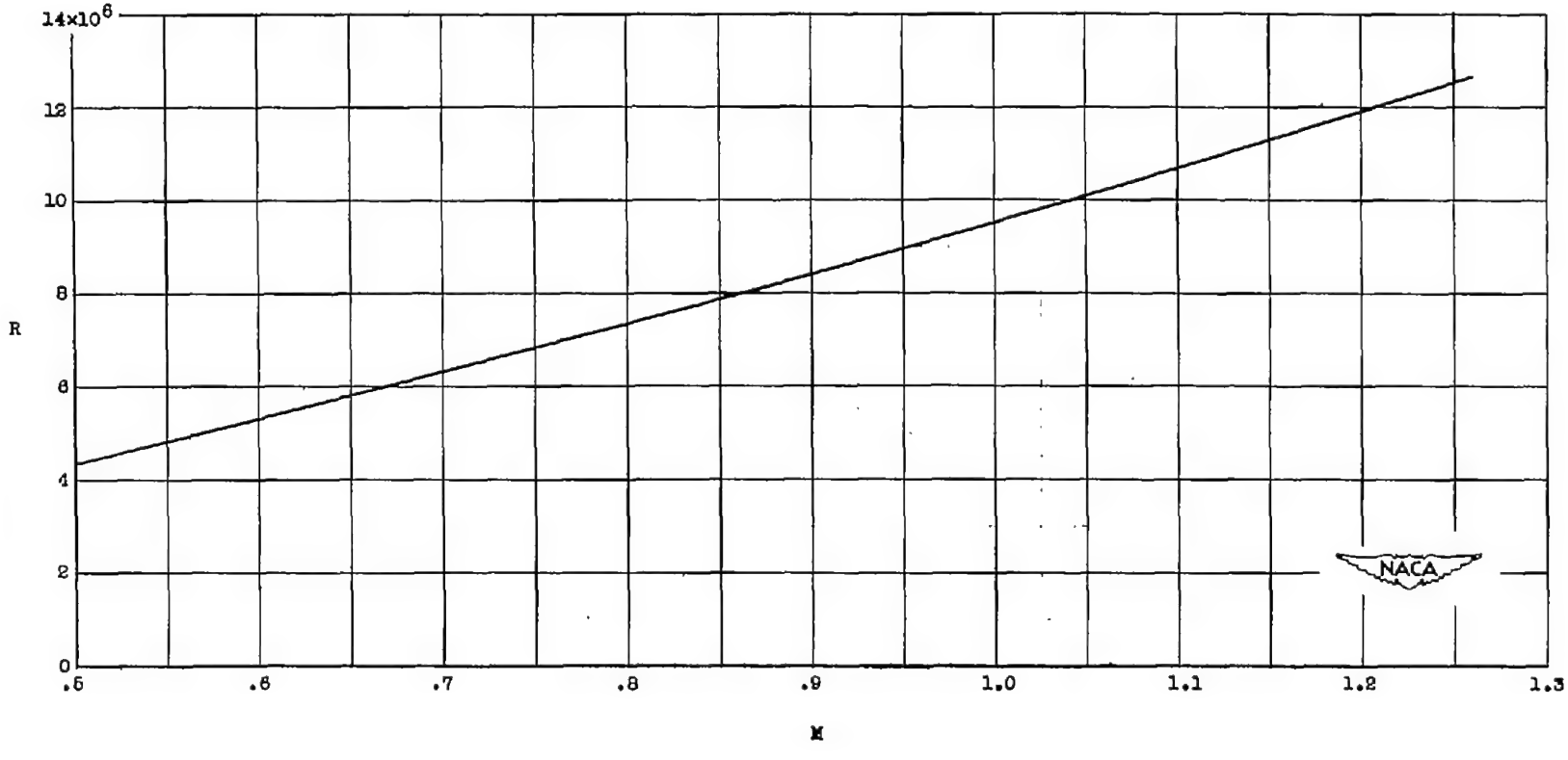

Figure 4.- Variation of Reynolds number with Mach number. Reynolds number is based on wing mean aerodynamic chord.

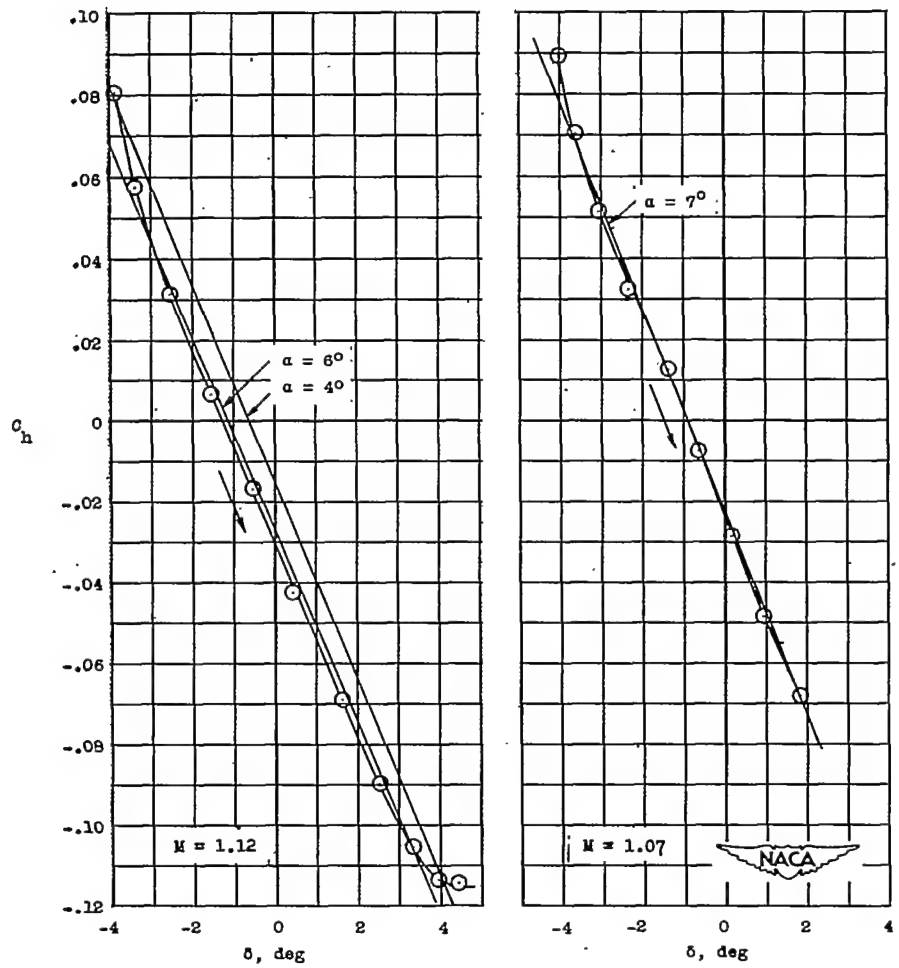

Figure 5.- Variation of hinge-moment coefficient with control-surface deflection at various angles of attack for Mach numbers of 1.12 and 1.07. Arrows indicate time sequence of recorded data.

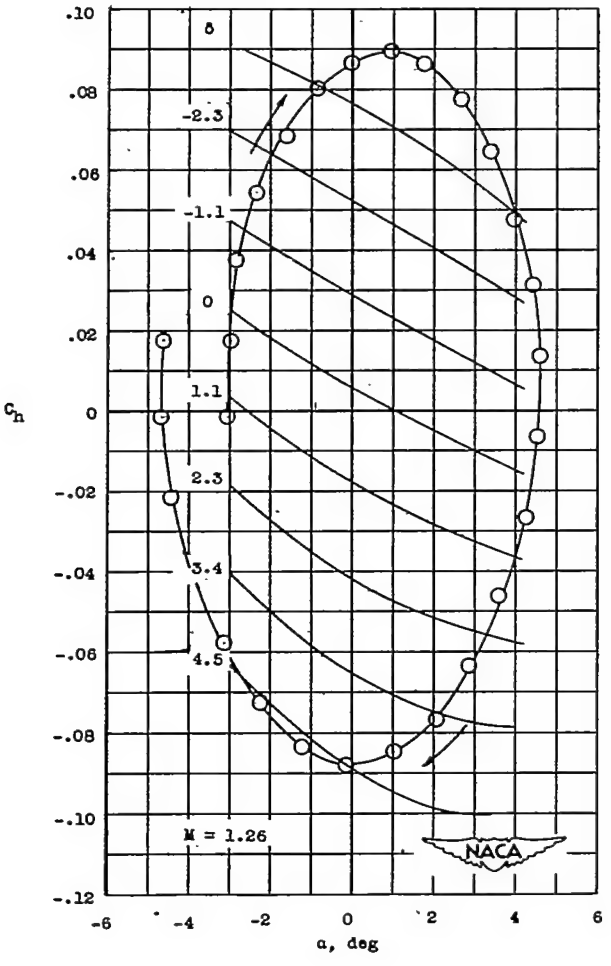

(a) M = 1.26.

Figure 6.- Variation of hinge-moment coefficient with angle of attack at various control-surface deflections between Mach numbers of 0.50 and 1.26. Arrows indicate time sequence of recorded data.

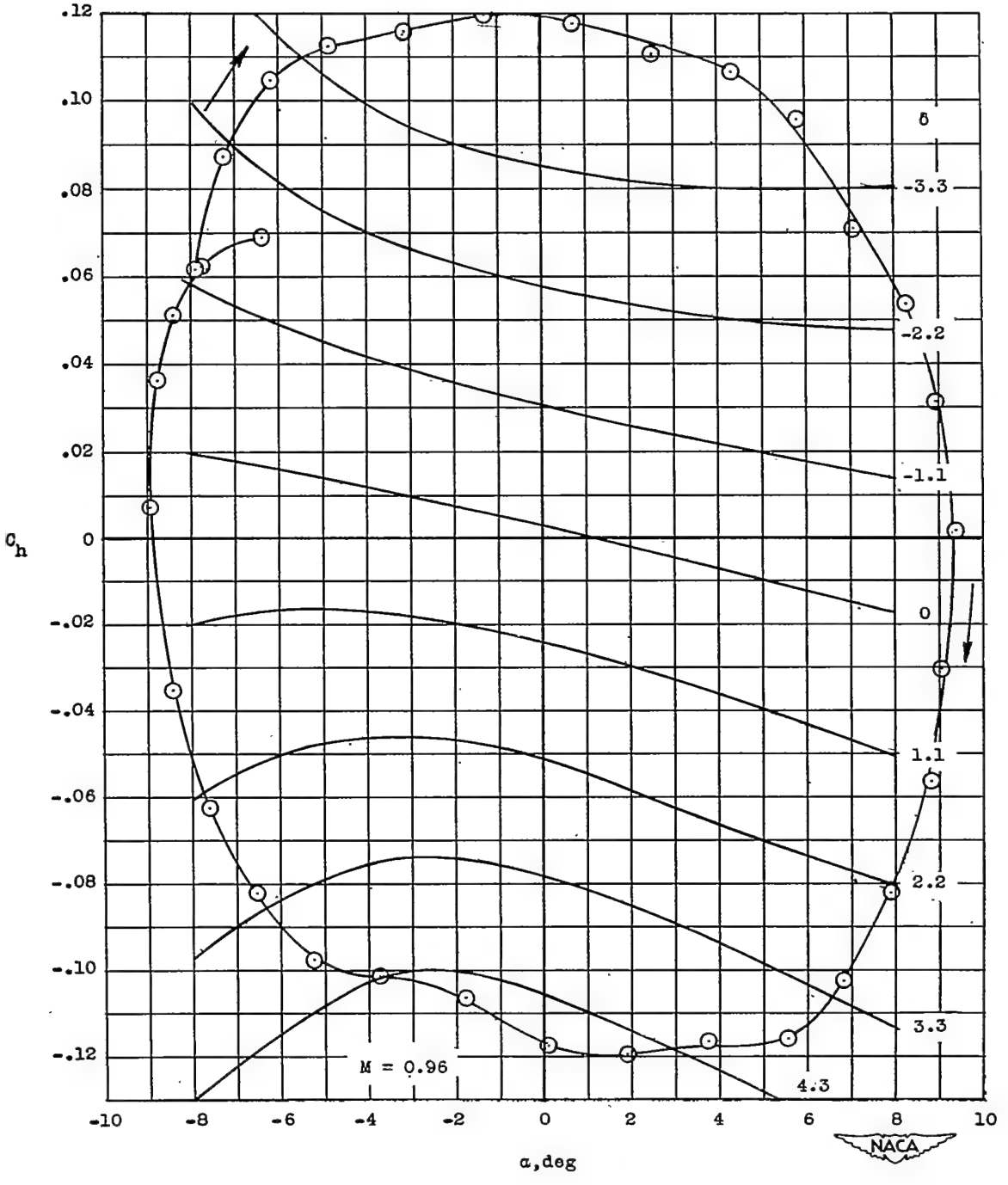

(b) M = 0.96.

Figure 6.- Continued.

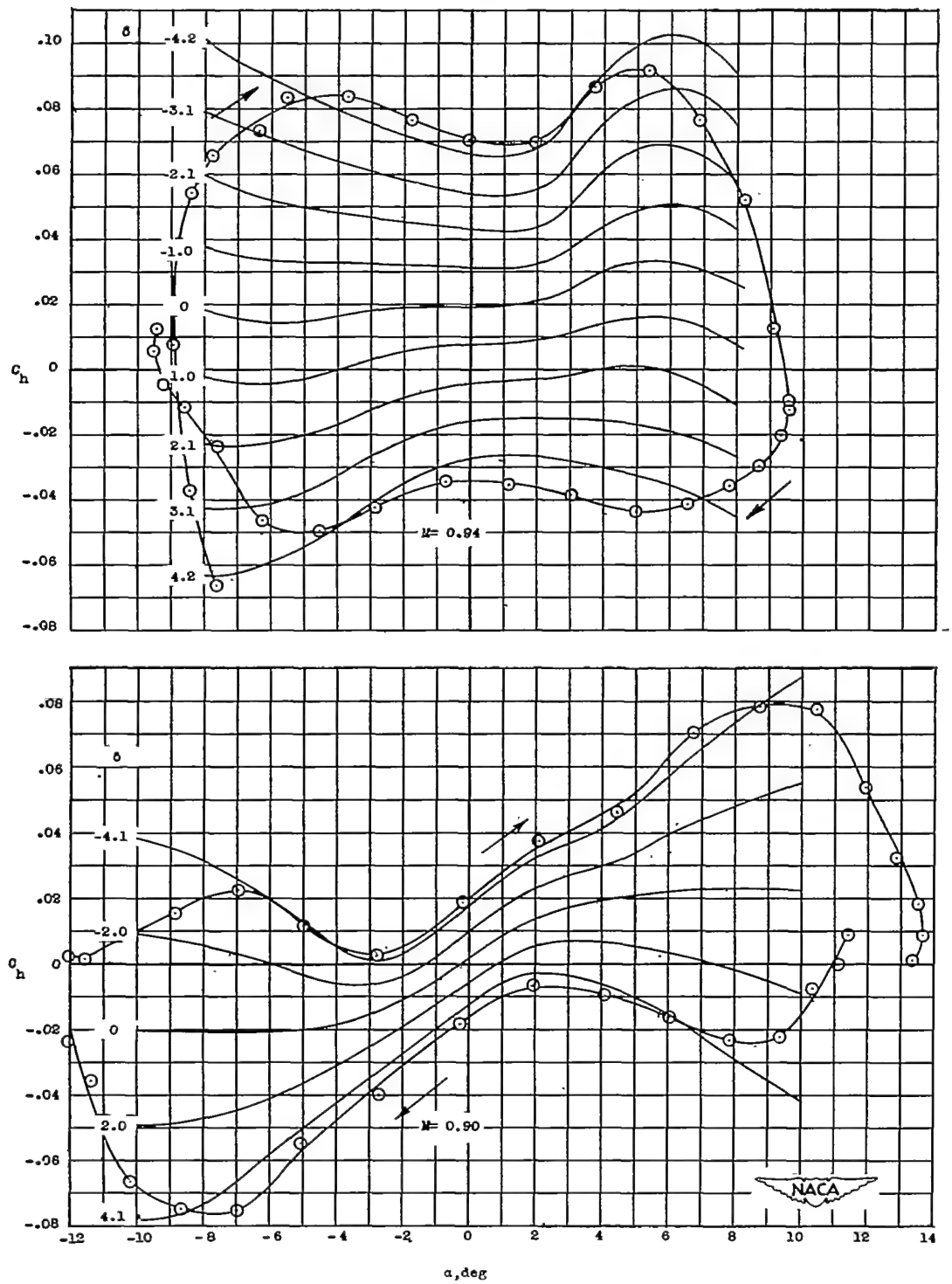

(c) M = 0.94 and 0.90.

Figure 6.- Continued.

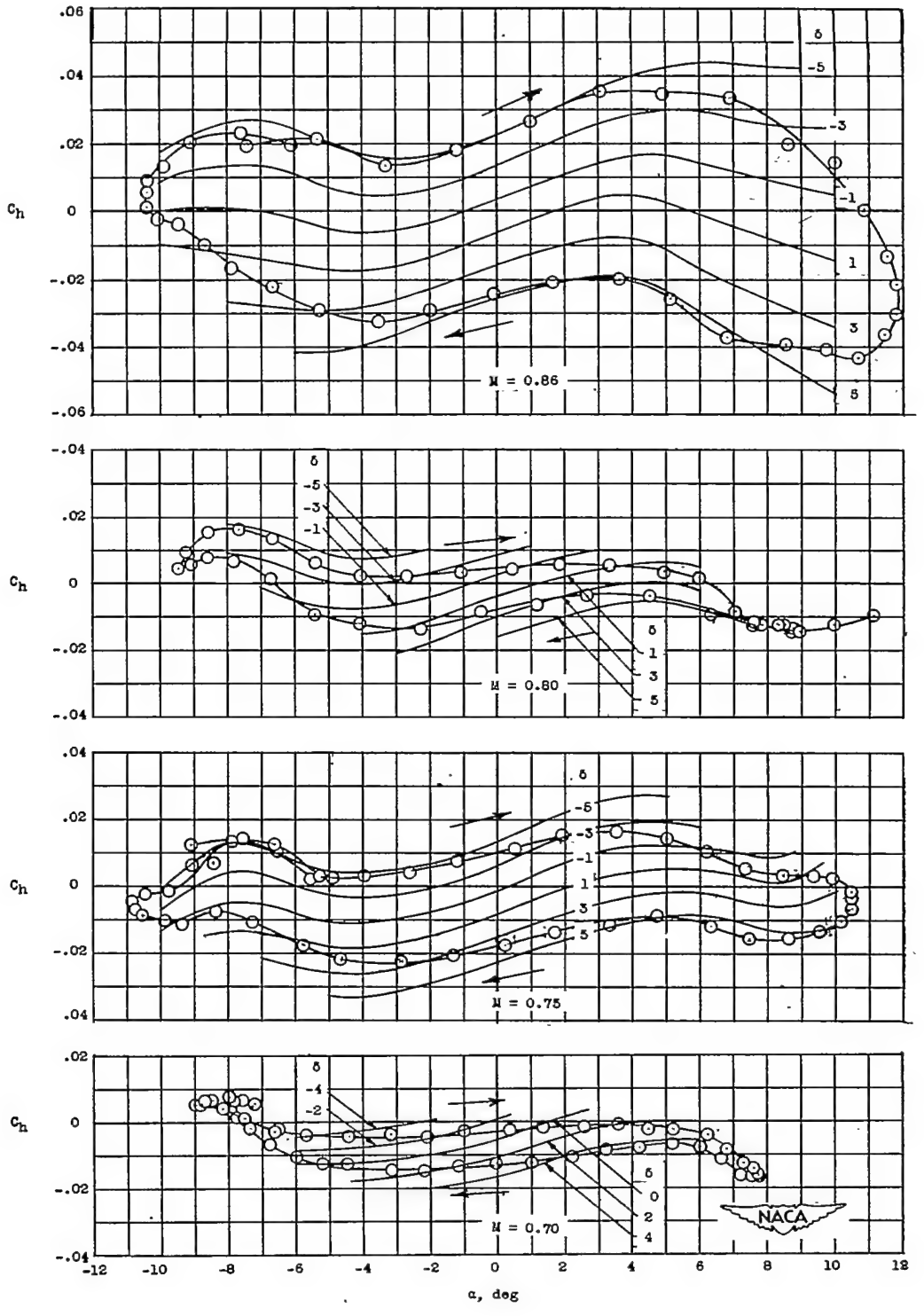

(d) M = 0.86, 0.80, 0.75, and 0.70.

Figure 6.- Continued.

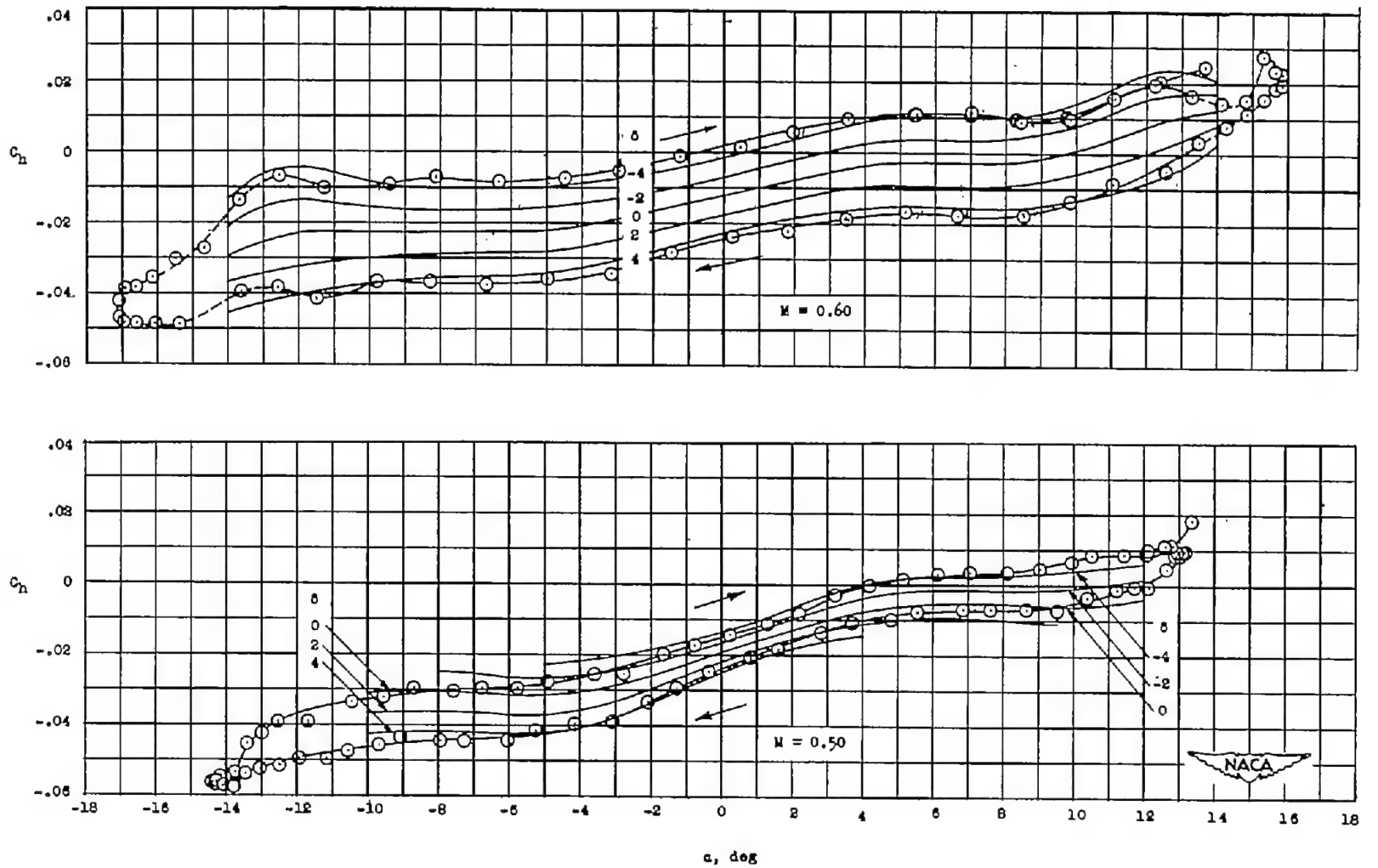

(e) M = 0.60 and 0.50.

Figure 6.- Concluded.

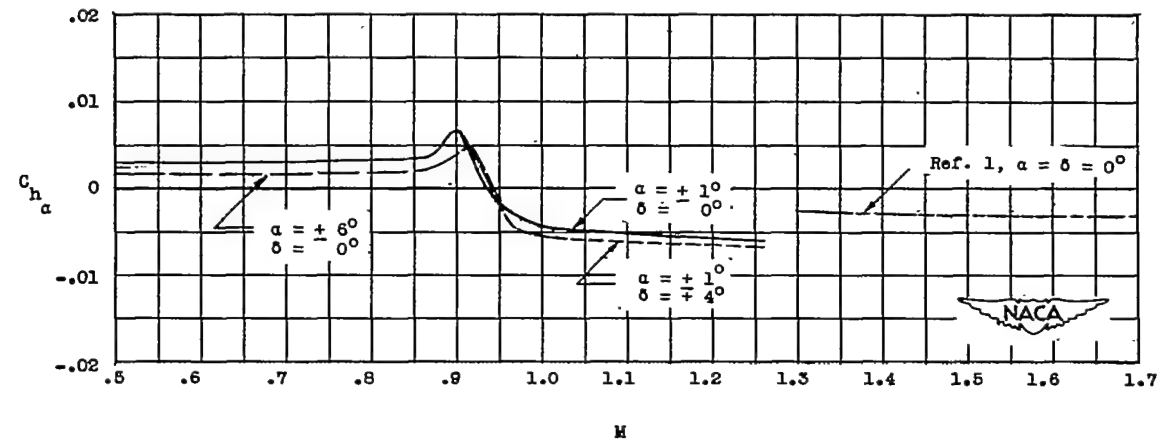

Figure 7.- Variation with Mach number of change in control-hinge-moment coefficient with respect to angle of attack.

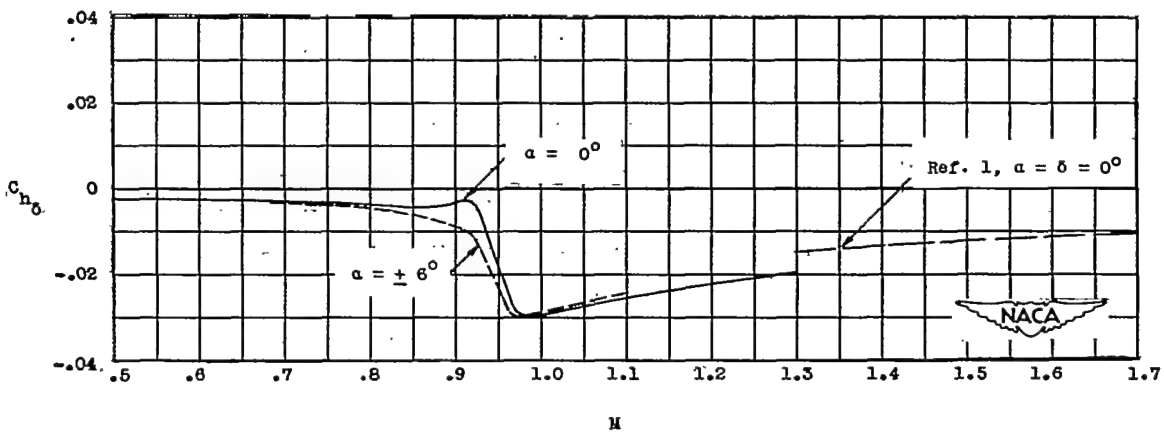

Figure 8.- Variation with Mach number of change in control-hinge-moment coefficient with respect to control deflection.

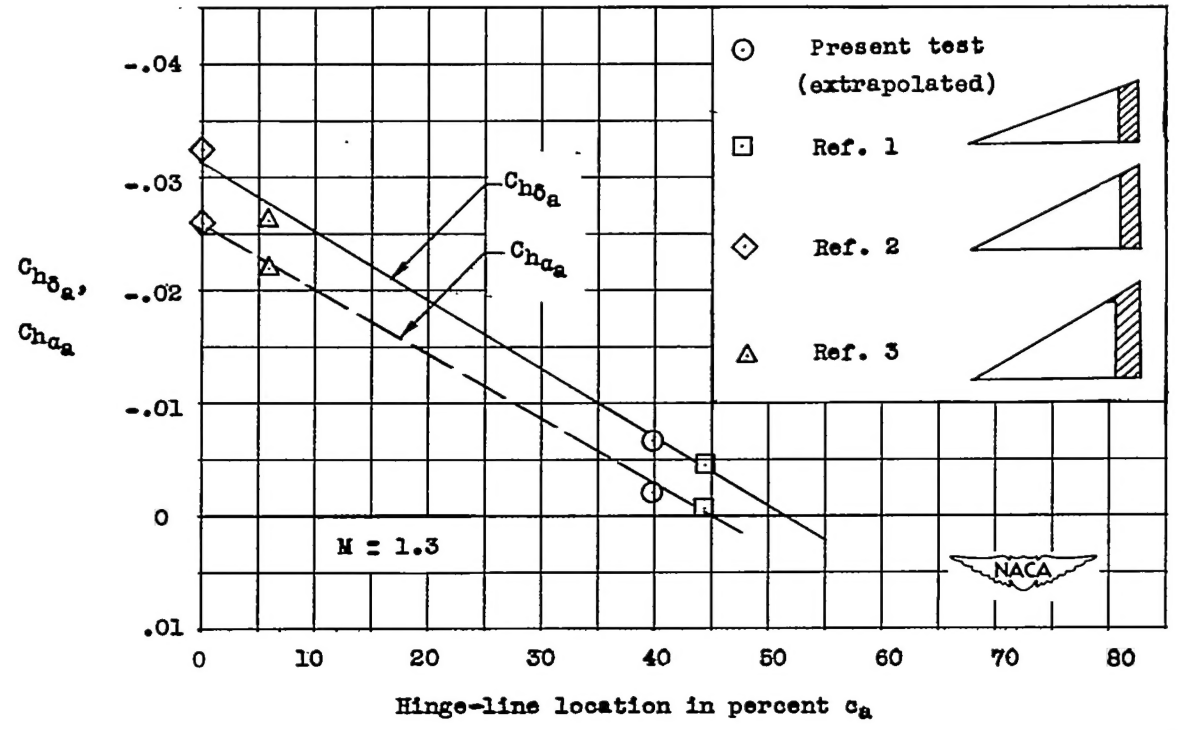

Figure 9.- Variation with chordwise hinge-line location of change in control-hinge-moment coefficient with respect to both angle of attack and control deflection at a Mach number of 1.3.

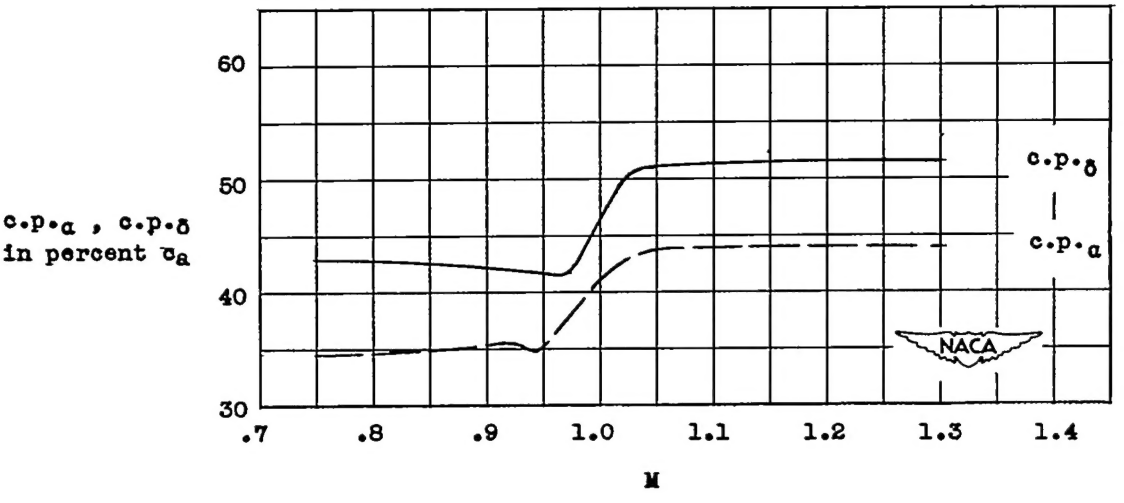

Figure 10.- Mach number variation of chordwise control center-of-pressure location as evaluated for control deflection and angle of attack.

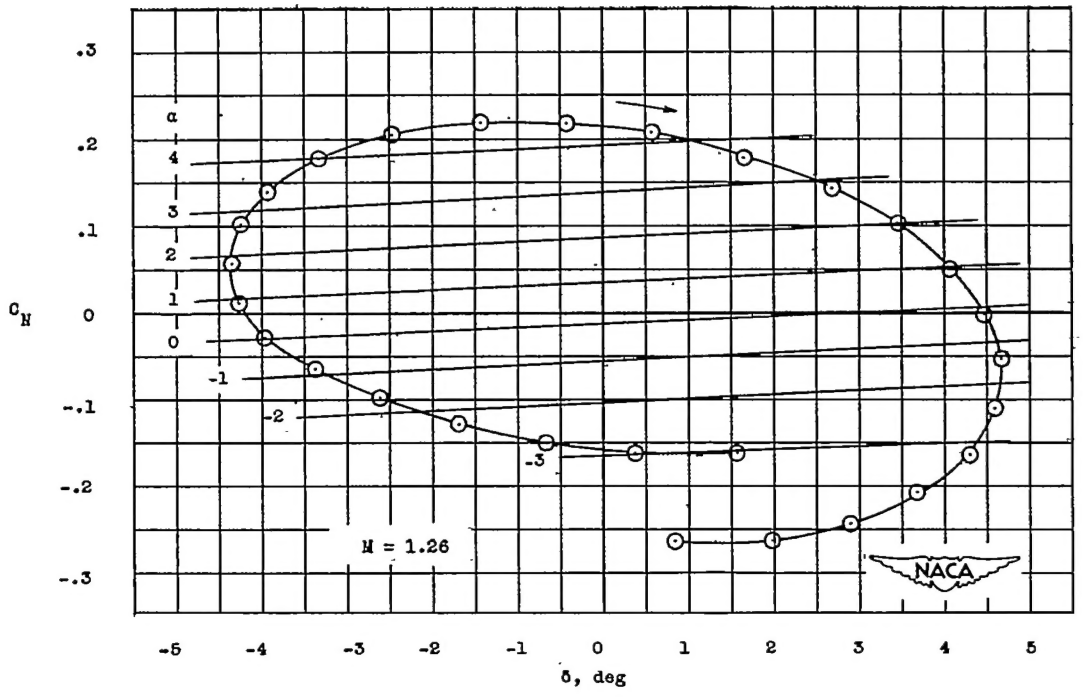

Figure 11.- Variation of normal-force coefficient with control deflection showing lines of constant angle of attack at a Mach number of 1.26.

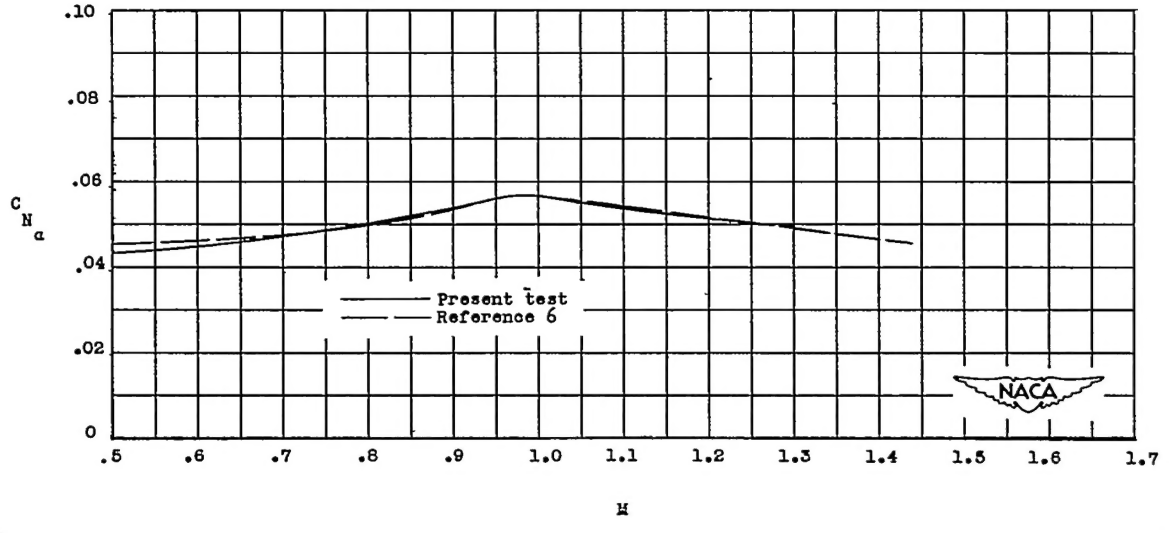

Figure 12.- Variation with Mach number of change in model normal-force coefficient with respect to angle of attack.

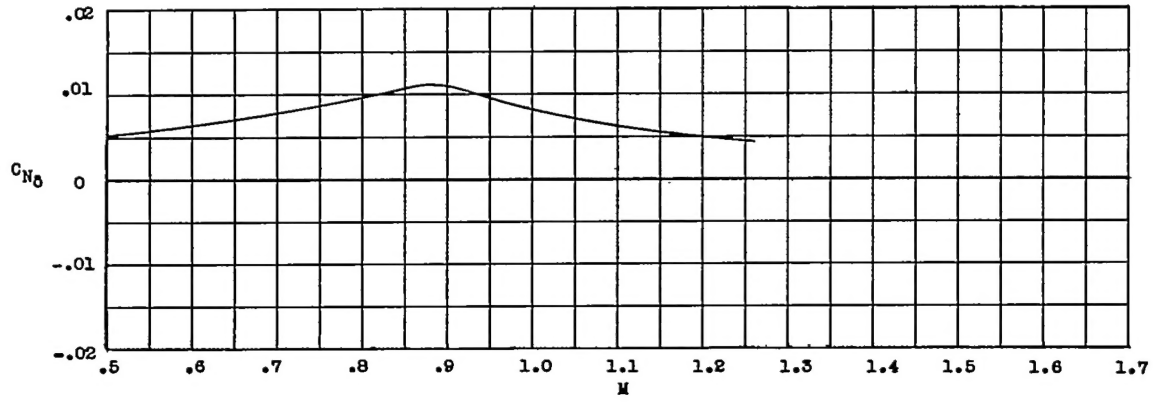

(a) Normal-force coefficient based on wing area.

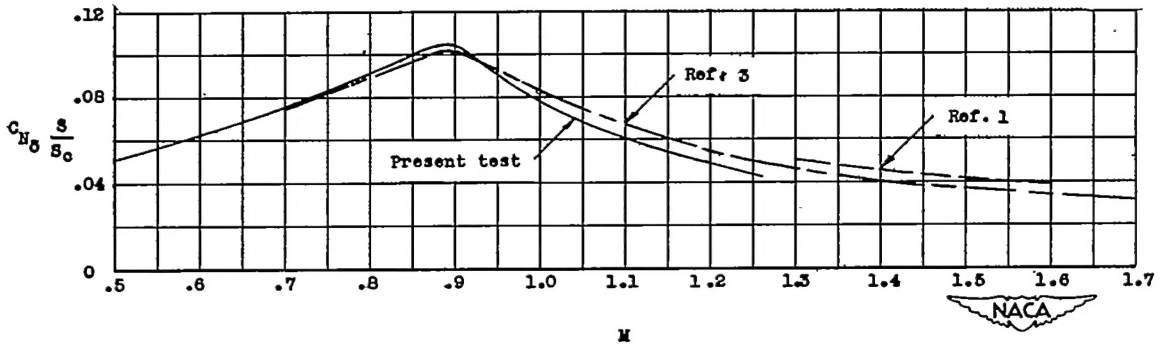

(b) Normal-force coefficient based on control area.

Figure 13.- Variation with Mach number of change in model normal-force coefficient with respect to control deflection.

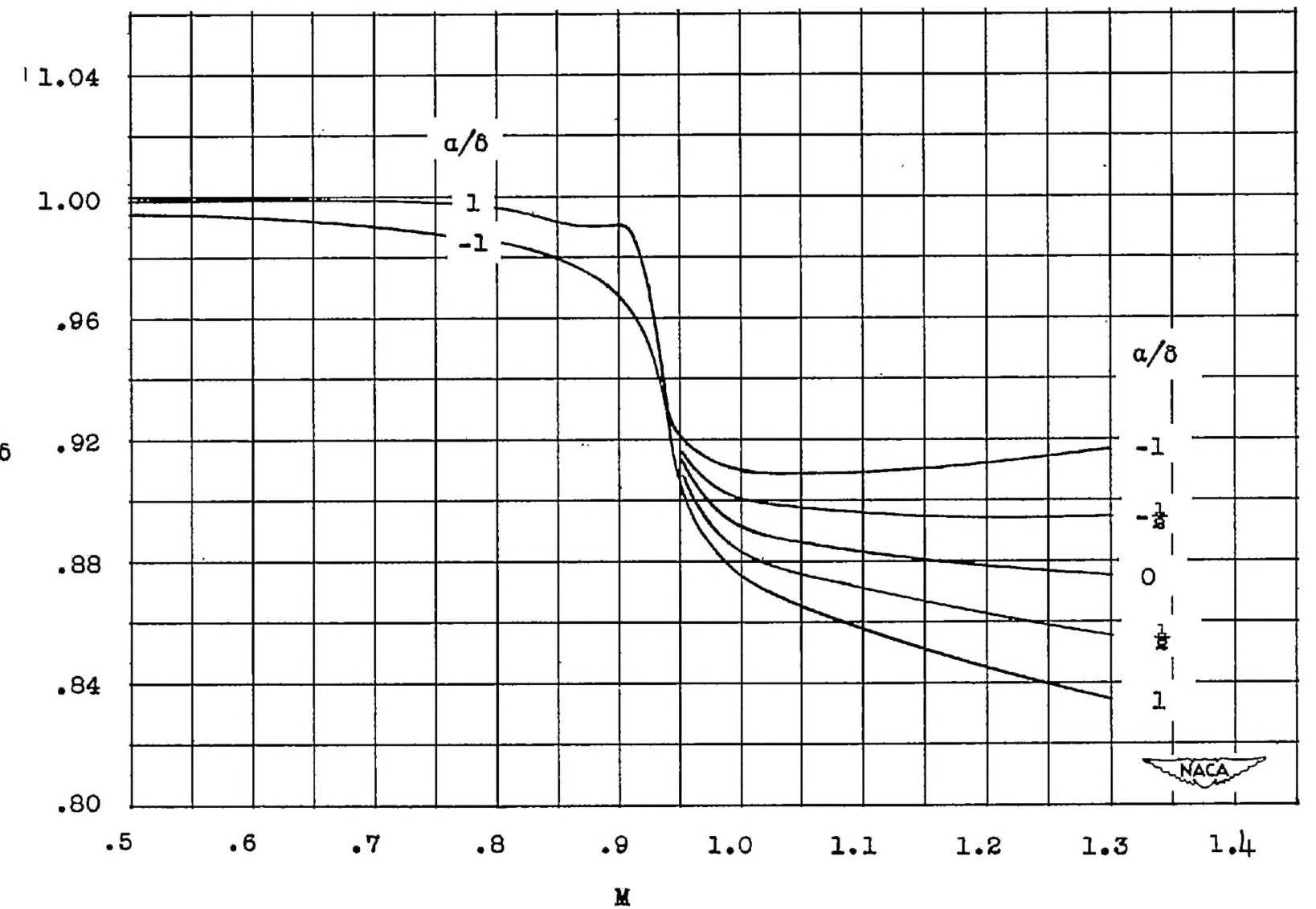

Figure 14.- Variation of control twist factor δ_e/δ with Mach number. Standard sea-level conditions. $H_o = 0$.